Martensitic transformation of Cu on Ag(001) and Cu on Au(001) studied with classical molecular dynamics

Z. S. Pereira and E. Z. da Silva
Institute of Physics "Gleb Wataghin," University of Campinas–Unicamp, 13083-970 Campinas, São Paulo, Brazil
(Received 13 October 2008; revised manuscript received 29 December 2008; published 4 March 2009)

The growth of Cu thin films on Ag(001) and Au(001) substrates was modeled using molecular dynamics with classical potentials. We observed that deposited atoms formed an unstable bcc or bcc/body-centered-tetragonal structure, in agreement with previous experiments. We show that the formation of such structures is related to film thickness and temperature that was analyzed in the interval from 200 to 600 K. bcc nucleation was measured by observing the relation between thickness and temperature of the deposited thin film. The martensitic transformation accompanied by a stripe pattern occurred as a consequence of the distortions caused by the underlying substrate lattice. The stripe patterns were measured as 57 and 61 Å for Cu on Ag and Cu on Au, respectively. Monolayer spacing and coordination number of atoms were calculated, clearly evidencing the formed structures. Local structures were studied using the Ackland-Jones method, to determine the phases of the deposited films.

DOI: 10.1103/PhysRevB.79.115404 PACS number(s): 68.55.−a, 68.35.Ct, 68.35.Rh

I. INTRODUCTION

Crystallographic face-centered-cubic (fcc) and body-centered-cubic (bcc) arrangements are the most common structures for metals. The description of such structures can be made using body-centered-tetragonal (bct) unit cells with lattice constants a and b ($a=b$) and different values of the ratio c/a; $c/a=1$ for bcc structures and $c/a=\sqrt{2}$ for fcc structures. One could therefore envision a continuum transformation from one to the other, fcc to bcc, for example. Arguments along those lines were suggested a long time ago. In 1924 Bain[1] suggested that fcc crystals could transform continuously into a bcc phase if subjected to biaxial expansion of a and b and compression along c axis on the order of 12%, changing the ratio c/a from $\sqrt{2}$ to 1 (see Fig. 1). A way to produce such a biaxial expansion and verify the proposal of Bain[1] is to grow thin metallic films on substrates with square symmetry and lattice constant approximately 12% larger than the fcc lattice parameter of the film, the substrate acting as a template for the new structure. The epitaxial growth and the phase transition in thin films are studied using various techniques such as electrodeposition, physical vapor deposition (PVD), scanning-tunneling microscopy (STM), surface x-ray scattering (SXS), and chemical beam epitaxy (CBE). This type of structural change is also known as martensitic transformation, observed experimentally in many works.[2–5]

First-principles calculations[6,7] have shown that the energy difference between fcc and bcc phases in Cu is only 20–38 meV. This evidences the possibility of obtaining bcc or bct Cu phase by deposition of Cu films on square symmetry substrates due to the tensile stress as proposed by Bain.[1]

In thin-film growth, deposited atoms can grow pseudomorphically, the first layer searching for the equilibrium positions of the substrate that have larger lattice parameter, an effect which causes stress, making a nonequilibrium structure more favorable than the natural one. As consequence of the martensitic transformation,[2–4] deformations emerge in the newly formed structure, such as stripes and in some cases a square-shaped moiré pattern and also an hexagonal moiré structure as observed in electrodeposition of Pb on Ag(100) or Ag(111).[8,9]

Stripe is a spatial modulated pattern closely related to the lattice mismatch, which appears, for example, in the growth of thin films of Cu on Ag and Cu on Au. Bittner *et al.*[8] showed that Cu deposited on Pt(100) has a pseudomorphic growth up to the tenth layer forming a bct phase. For larger thickness the Cu relaxes to a bulk structure and a moiré pattern is formed.

We used molecular dynamics (MD) as implemented in the software LAMMPS (Ref. 10) to study two systems: Cu deposited on Au(001) and Cu deposited on Ag(001). Electrodeposition, the experimental technique used in the film growth of Cu in Ag (Ref. 4) and Cu in Au,[2] produced a layer-by-layer type behavior. We therefore modeled our computer-simulated growth accordingly, obtaining also a layer-by-layer growth. Both systems present similar results according to previous experimental reports.[2,4] The interaction of deposited Cu on Ag and Au was modeled with embedded-atom method (EAM),[11–13] and the structure determination was performed using the Ackland-Jones method (AJM).[14] Previous theoretical works have discussed initial stages of growth of Cu on Ag(001), Pt on Au(100), and Au on Pt(100).[15,16]

It is worth stressing that the existence of bcc and bcc/bct phases observed in growth of thin films is related to tempera-

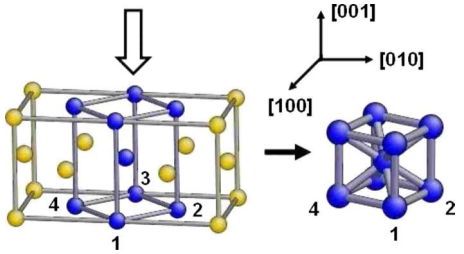

FIG. 1. (Color online) Schematic representation of the martensitic transformation proposed by Bain (Ref. 1). A fcc lattice subjected to biaxial expansion in a and b transforming into a bcc lattice.

ture and the Cu film morphology is strongly influenced by the structure formed at the interface with the substrate.[3] Our results help in understanding qualitatively and quantitatively the relation of temperature and bcc/bct formation in the Cu film at specific nucleation thicknesses. For some chosen thicknesses the ratio of bcc nucleation (bcc-nucleated atoms per total deposited atoms) of deposited atoms after annealing was analyzed with a discussion of the relationship between film temperature, thickness, and formed structures. Cu/Ag(001) and Cu/Au(001) systems were studied.

Figure 1 presents a schematic representation of the martensitic transformation. The fcc structure with base formed by atoms 1–4 expand in the [100] and [010] directions with a simultaneous compression in the [001] film growth direction, transforming into a bcc structure. Note that the crystallographic axis of the formed bcc phase does not coincide with the crystallographic axis of the fcc substrate. Now the [100] and [010] are rotated by 45°.[17] Therefore the Cu[001] direction is parallel to the [001] direction of Au and Ag, and the Cu[110] is parallel to the Au and Ag [100] direction. The mechanism just described will be discussed in the simulations presented in this paper.

The plan for this paper is as follows: in Sec. II we discuss the computational procedure and the methods for analyzing the data. Section III shows the results for the system Cu on Ag, and Sec. IV presents the results for the system Cu on Au. Section V presents conclusions and perspectives for future work.

II. COMPUTATIONAL PROCEDURE

Here we discuss details of the potential used in the present calculations and continue with details of the simulations performed and the methods used to analyze the results that give evidence for the martensitic transformation occurring during the Cu film growth.

A. Potential

The interaction of different metallic species was modeled by the EAM. This interatomic modeling was initially proposed by Daw and Baskes,[11,12] and subsequently Foiles *et al.*[13] showed that it could be used for alloys and mixtures of metals. This potential is based on the density-functional theory (DFT) (Ref. 18) and on the idea that the total electronic density of a metal can be approximated by a linear superposition of the densities of each atom. The mathematical basis of EAM comes from the corollary proposed by Stott and Zaremba[19] which states that the energy of an impurity in a metal host is a functional of the electronic density of the system without the impurity, or that the embedding energy of an impurity is obtained from the electronic density of the host before the impurity is added to the system. In this approach each atom is treated as an impurity embedded in the host composed by all the other atoms. The potential is constructed semiempirically for metals and mixtures of these metals such as Cu, Ag, Au, Pd, Pt, and Ni (Ref. 13) and also alloys such as AlCu (Ref. 20) or CoAl.[21] In this paper we use exactly the same functions that were determined and tabulated for interactions between pure metals and their alloys in agreement with Refs. 12 and 13.

The total energy is given by the sum of the functional of the density (embedding energy) for a site, without considering the impurity, plus the pair electrostatic interaction of the impurity with the atoms from the local environment. The equation for the total energy is

$$E_{\mathrm{tot}} = \sum_i F_i(\rho_{h,i}) + \frac{1}{2}\sum_{i,j(i\neq j)} \phi_{ij}(R_{ij}). \quad (1)$$

F is the embedding energy which is a function of the electronic density ρ, and ϕ is the pair potential. Both sums are over all neighbors j of atom i inside a cutoff distance. The many-body nature of the EAM potential comes from the embedding-energy term. It is important to note that the embedding function F does not depend on the source of the electron density of the host (background electron density). Therefore the same embedding function (F) can be used to calculate the energy of an atom in a pure metal or in an alloy.

The functions F and ϕ are fitted to reproduce exactly the equilibrium lattice constant, the sublimation energy, elastic constants, and vacancy energy formation for pure metals and the heats of solutions of the binary alloys.[13] This procedure to fit F and ϕ, giving the sublimation energy and elastic constants, makes EAM a good theory for problems of expansion and compression of bulk metals since these expressions give good fits to the equation of state and consequently reproduce accurately mechanical properties of many metals, which justify the use of EAM in the present calculations.

B. Simulations and the Ackland-Jones method

The initial geometrical construction of the structures for the simulation is similar for both systems studied. For Cu deposited on Ag and Cu deposited on Au, a substrate of dimensions $13.9\times13.9\times2.45$ nm^3 with 26 624 atoms was used. We used periodic boundary conditions for the lateral faces, while the growth direction was left free from constraints except for the bottom layers that were kept frozen. Tests were performed with one and three fixed bottom planes with similar results. The substrate thickness was 13 layers and was sufficiently large for the present work. The Verlet algorithm was used to integrate the equations of motion in the canonical ensemble where the substrate temperature was kept at 300 K using Nose-Hoover thermostat.[22] The basic idea of the Nose-Hoover method is to couple the Hamiltonian of the system to virtual thermostats that interact with the system exchanging energy with a thermal bath and therefore keeping the temperature constant throughout the simulation. A neighbor list was constructed with a cutoff radius of 6 Å and updated each time any atom of the simulation moves more than 1 Å.

The simulated growth process of Cu on Ag(001) and Cu on Au(001) occurs randomly. The deposition of an atom in a position in the {001} plane above the top layer is chosen arbitrarily, as well as the initial height and the particle velocity, which varied between the intervals of 2.5–3.0 Å and 0.12–0.20 Å/ps, respectively. The initial height of the deposited particle takes into account the highest previously de-

posited particle. This procedure guarantees that deposition is layer by layer. Initially deposited particles are not in the equilibrium imposed on the substrate since the simulation increases the number of particles with time, with 1 ML deposited at each 102.5 ps. The force felt by each particle during deposition was calculated from the interaction potential and the equations of motion were integrated using Verlet algorithm. In this sense the substrate also behaves as a heat reservoir for the deposited atoms. During deposition a 2 fs time step was used. After all atoms were deposited the time step for annealing of the whole system was 1 fs to take the whole system to a more relaxed structure. The growth process, as in the experiments, due to the moderate strain posed by the substrate, allowed the layer-by-layer growth instead of a cluster growth.

We performed analysis of 11, 13, 14, 15, 18, and 20 ML of Cu on Ag and Au. After deposition, the system was relaxed by annealing, and the entire system temperature was gradually ramped from 300 to 600 K in 300 ps with a 1 fs time step. It was then maintained at 600 K for another 200 ps and was finally linearly reduced to 200 K in 400 ps, which corresponds to a rate of 1 K/ps. The time step for annealing was 1 fs. The total simulation times for deposition plus annealing for the thicknesses described above were 2.0, 2.2, 2.3, 2.4, 2.7, and 3.0 ns. With the system relaxed the local structure was determined with the Ackland-Jones method for a selected set of structures at each temperature.[14]

The AJM distinguishes between bcc, fcc, and hcp structures and can be implemented to analyze structures using the local distances or angular distribution. In the present analysis only atomic positions were necessary. The method is based in the analysis of the radial and angular distribution functions of perfect-crystalline lattices as well as lattices with small distortions due to temperature and that are generated in the simulations. From a heuristic algorithm[14] it is decided which type of local environment is attributed to each particle. The method is limited to a number of structures of interest in a given application. It was chosen because it is adequate for describing martensitic transformations that show lattices largely distorted from the perfect lattice.[14] Another advantage of the AJM is in the identification of structures with periodic boundary conditions; all atoms are distributed correctly in their surroundings. The method sometimes fails to identify the structure of a particular atom. That atom is marked as unknown; this can occur for atoms at surfaces and structures not described by the method.

We also analyzed the coordination number of each atom based in a cutoff distance for the first-neighbor distance. This method is not efficient at high temperatures, although at room temperature it gave a good indication of the coordination number and the first-neighbor distance for the Cu-deposited film, suggesting that a new phase was formed. The local structure was decided by the Ackland-Jones method.

For the thicknesses previously described, we used the AJM to calculate the ratio of bcc nucleation (bcc nucleation per deposited particle) as function of temperature in the 200–600 K temperature interval. We excluded from this analysis the interface Cu/Ag and Cu/Au atoms and the top-layer Cu atoms that cannot be treated by the AJM.

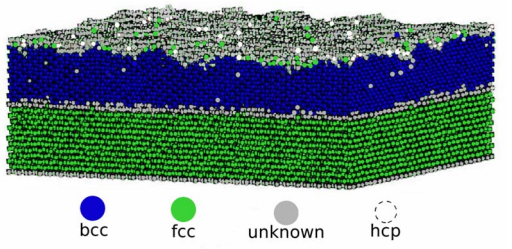

FIG. 2. (Color online) The structural transformation of Cu on Ag with the use of AJM for a Cu film with 15 ML at 360 K. The atoms colored blue (dark gray) indicate the formation of a bcc phase, therefore showing that the deposited Cu film is in a bcc phase; green (light gray) atoms indicate a fcc phase (substrate Ag); white means hcp; and gray indicates atoms that the AJM failed to identify their structures.

III. RESULTS AND DISCUSSION: Cu ON Ag

A. Martensitic transformation and distances between monolayers

Cu deposited on Ag substrate at room temperature has a layer-by-layer growth as specified in Sec. II. Cu grows in a bcc structure for the first few layers, but depending on temperature and thickness the phase can become bct or even fcc, as also observed in experiments.[2,4] Under these circumstances, the Cu film undergoes a martensitic transformation accompanied by a modulated stripe pattern. We discuss also the relation between film thickness, temperature, and the formed bcc and bct structures. To exemplify this fact we show in Fig. 2 the structural change in the Cu film with 15 deposited monolayers at 360 K using the AJM. At lower coverage even at lower temperatures the bcc structures are stabilized. For example, for 10 ML at 300 K the bulk of Cu is still nucleated in the bcc phase. Note that at the Cu/Ag interface the majority of the atoms are not identified by the AJM (colored gray). This is explained when we calculate the interplanar distance of the Cu/Ag interface and Cu/Cu in the bulk of the Cu film. Taking into account the average distance of atoms in two adjacent monolayers that form the interface, the calculated interlayer (001) distance for the interface Cu/Ag was 1.73 Å, while for Cu/Cu interlayer distances a value of 1.41 Å was obtained, which is different from the interlayer distance for fcc Cu that should be 1.81 Å. Therefore it indicates that Cu is compressed in the growth direction, giving evidence for the structural change. This result is in agreement with the experimental value of 1.4 Å obtained for the interlayer distance along the direction [001] for the Cu film, given by Dietterle *et al.*[4] The majority of the top-layer atoms are colored gray; the method cannot identify such structures. It is known from first-principles calculations[6,7] that the most stable Cu structure is fcc. But the present results indicate that under expansion of the *a* and *b* directions, Cu reorganizes to form a bcc phase which is the structure that gives the energy minimum under these circumstances.

B. Stripes

The martensitic transformation is further verified due to the stripe formation. In the case of the Cu/Ag(001) system,

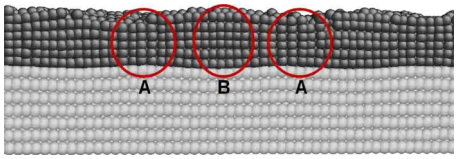

FIG. 3. (Color online) Buckling caused by the structural change in the Cu film with 11.5 ML at 300 K. For the purpose of visualization a plane cut normal to the [110] direction was used. The colors light and dark gray are used to represent Ag and Cu, respectively. The picture from the simulation was cut at the sides for better visualization.

this formation starts between the ninth and the tenth deposited layers. Before no pattern is observed, which indicates that the strain in the lattice is relieved at the interface only after nine deposited layers, also in agreement with the experimental findings of Dietterle *et al.*[4]

The transformation of fcc Cu continuously into bcc Cu, without volume change, should occur when the film is subjected to biaxial expansion of a and b directions by 12.2%. For Cu on Ag(001) the lattice mismatch is 13%. The film grows pseudomorphic to the substrate but after a critical thickness it relaxes, creating a deformation pattern leading to the formation of stripes associated with the nucleation of bct (fcc) and bcc phases. We measured the surface-normal compressive strain for the cooper film using the expression[23]

$$\Delta = \frac{d_{\text{film}} - d_{\text{bulk}}}{d_{\text{bulk}}}, \tag{2}$$

where d_{film} and d_{bulk} are the interlayer distances of the film and the bulk Cu, respectively. This calculation was made both during the growth of the film, up to the eighth monolayer, and after the formation of the stripes, above 9 ML at 300 K. We verified that during the growth the compression was approximately constant throughout the film, with $\Delta=-21\%$, and the Ackland-Jones method showed that the structure of the film was bcc. But between the growth of the ninth and the tenth monolayers, the compression values changed suddenly. Furthermore, a buckling appears throughout the film as can be seen in Fig. 3, which shows regions of low compression, where $\Delta=-12.7\%$ (region B in Fig. 3), and regions of high compression, $\Delta=-27.6\%$ (region A in Fig. 3). Therefore the stripe pattern formed (see also Fig. 4) is consequence of the compression changes throughout the film. This effect is also shown in Fig. 4, which presents the interface Cu layer for increasing number of deposited Cu layers. Note that the modulated pattern occurred only after the deposition of the ninth layer, further evidencing the martensitic transformation that occurs in Cu deposited on Ag. Therefore, the bcc nucleation was significantly reduced when the formation of stripes occurred because of the deformations found in the film.

Figure 4 shows the evolution of the pattern formed in the first monolayer/interface after deposition of 8, 9.5, 10, and 11 ML at 300 K; atoms above this layer were made invisible. Figure 3 displays the buckling pattern of the stripes that are related to the compressive strain in the growth direction. For the purpose of visualization, a plane normal to the [110] direction of the stripes was considered. The measured stripe period was estimated using the first deposited layer as 57 Å. Stripes can orient themselves, forming 90° domains[4] in this case. Both directions, [110] and $[\bar{1}10]$, are energetically favorable and symmetrical. Because of the areas of the system studied (13.9×13.9 nm^2), we observed the formation of one stripe domain. We estimate from the experimental data of Ocko *et al.*[2] and Dietterle *et al.*[4] that, in order to observe the formation of more than one stripe domain, it would be necessary to simulate a system with an area of 100×100 nm^2.

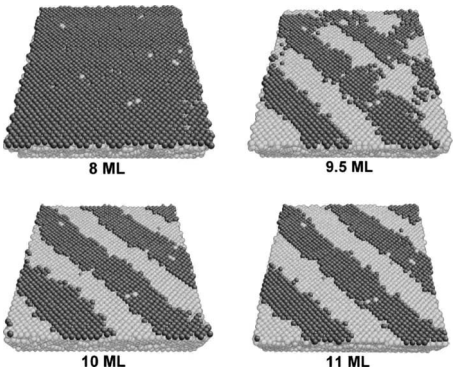

FIG. 4. Evolution of the stripe pattern formed at the interface. Images show the first Cu monolayer on Ag (atoms from layers above the interface are made invisible). After the deposition of the ninth layer, the film starts to show stripes, corroborating the martensitic transformation. The colors light gray and dark gray are used to represent Ag and Cu, respectively.

C. Relation of temperature, film thickness, and bcc/bct structures

The formation of different phases, namely, bcc, bct and fcc, is related to the temperature and thickness of the film. The change in temperature causes volumetric expansion or contraction, and is clearly related with the deformations found in the deposited Cu film. Figure 5 shows the percentages of bcc nucleation of Cu for different numbers of deposited layers (11, 13, 15, and 20 ML) as function of temperature. The film with 15 layers at 360 K shows that most of the film (96.29%) is nucleated in the bcc phase, but at 350 K a drop in the bcc nucleation (56.54%) occurs. At a fixed thickness the Cu film showed different ratios of bcc nucleation, when the temperature varied from 600 to 200 K. For all thicknesses analyzed there was a range of temperatures in which the structures were predominantly bcc. At 13 ML, in the range from 340 to 600 K, more than 90% of deposited Cu was identified as bcc. On the other hand, from 200 to 330 K the amount of atoms identified as bcc was significantly smaller (55% at 200 K). At 15 ML, bcc nucleation above 90% was verified between 360 and 600 K, but below this temperature a significant drop in the bcc nucleation occurs, reaching a measured value of 35% at 200 K.

Lowering the temperature increased the quantity of bct-nucleated atoms causing lattice deformations. A considerable drop in the number of Cu atoms with bcc structure occurs with formation of a bct phase, with coexistence of both

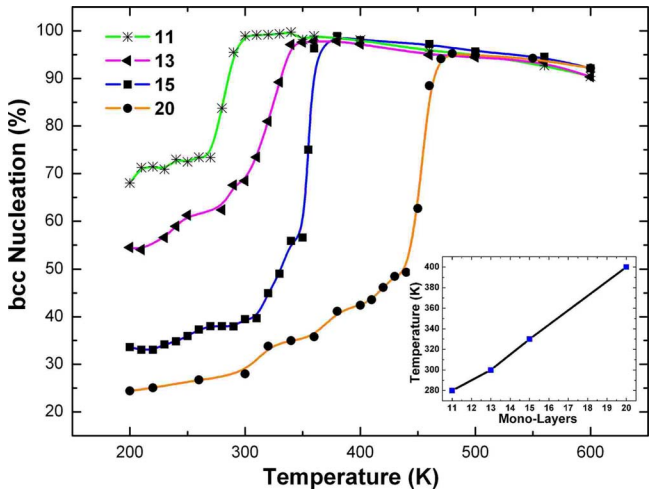

FIG. 5. (Color online) Percentages of bcc-nucleated atoms as function of temperature, after deposition of 11, 13, 15, and 20 ML of Cu on Ag. Interface and top-layer atoms were not taken into account since the AJM could not identify them. The inset presents the transition temperature of the bcc to bct as function of the thickness.

phases. The tetragonal formed phases are structures that were previously bcc and had suffered deformations caused by temperature. Initially, in the first Cu layers the growth is pseudomorphic. But with the deposition of many layers, at a given temperature the tensile biaxial stress in a and b is reduced, consequently reducing these parameters, while along c it increases, consequently relaxing the Cu superior layers into a more relaxed structure (bct $\rightarrow$ fcc). This is a trend for the Cu bulk structure with the deposition as the number of layers increases. The fcc phase appears above 20 ML in the case of Cu on Ag.[4] It is worthwhile to note that the drop in the ratio of bcc nucleation is much smaller for 11 ML at 200 K, compared with the one for 20 ML at the same temperature. This shows that at 11 ML the biaxial tensile stress in a and b acts in the whole deposited film, still keeping the pseudomorphic growth. On the other hand, the larger the thicknesses are, the lower the stress is, explaining the small variation in the bcc nucleation ratio with varying temperature. The inset of Fig. 5 shows that the transition temperature from bcc to bct structure is approximately linear with the number of Cu-deposited layers. This means that for larger film thickness up to 20 ML, the temperature of at which the drop in bcc nucleation had occurred was proportional to the number of deposited layers, being approximately 280 K for 11 ML and 330 K for 15 ML. The temperature was determined as the mean value of temperatures just above and just below the large drop on bcc nucleation.

IV. RESULTS AND DISCUSSION: Cu ON Au

A. Martensitic transformation and distances between monolayers

Cu deposited on Au is very similar to the system Cu/Ag(001) discussed previously. The lattice mismatch is 12.9%, very close to the value in the case of Cu on fcc Ag

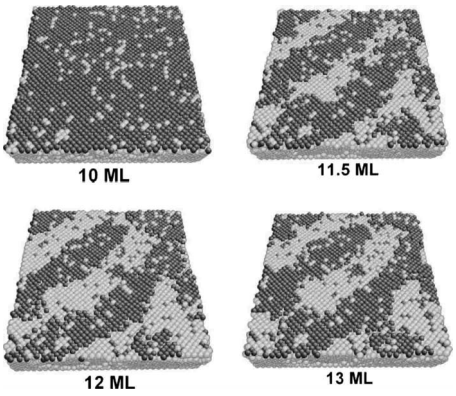

FIG. 6. Evolution of the stripe pattern formed at the interface. Images show the first Cu monolayer on Ag (atoms from layers above the interface are made invisible). After the deposition of the 11th layer, the film starts to show stripes, corroborating the martensitic transformation. The colors light gray and dark gray are used to represent Ag and Cu, respectively.

(13%) and again not far from the Bain proposed value of 12.2%. In this case we observed the pseudomorphic growth and the martensitic transformation to the bcc phase with the Cu deposition on Au(001). The overall behavior was very similar to the structure presented in Fig. 2 and was analyzed with AJM. In the deposition of Cu on Au, even at 320 K the whole bulk of the Cu film was nucleated bcc up to 11.5 ML. The interlayer distances in the (001) direction were 2.0 Å for Au-Au, 1.67 Å for the interface Au-Cu, and 1.38 Å for Cu-Cu in the bulk of the thin film.

B. Stripes

Cu on Au formed stripes in a similar way as in the previous case of Cu on Ag. In the case of Cu on Au, the stripe formation started after deposition of more than 11 ML as shown in Fig. 6, which presents the evolution of the stripe pattern formation as Cu layers were deposited. Similar to the case of Cu on Ag, the surface-normal compressive strain was calculated and we found that during the growth, the compression was approximately constant throughout the film, with $\Delta=-19.33\%$ up to 11 deposited layers. After that, the film started to show regions of low compression, $\Delta=-15.5\%$, and regions of high compression, $\Delta=-24.9\%$. The periodicity of the stripe pattern for the present case was estimated at 61 Å, in good agreement with results of Ocko *et al.*[2] that observed periods of 60–75 Å. As discussed before in the case of Cu on Ag, stripes can orient themselves, forming 90° domains,[4] and both directions, [110] and [$\bar{1}$10], are energetically favorable. We found the formation of stripe domains in the [$\bar{1}$10] direction, but in this case the direction of stripe pattern was rotated by 90° in comparison to the system Cu on Ag (see Figs. 4 and 6). Our system is small (13.9×13.9 nm^2) to ascertain the formation of stripes in more than one direction in one simulation. Study of larger structures is out of the scope of the present simulations.

Experimental results as well as the present work found a stripe pattern more largely spaced for the Cu/Au than for

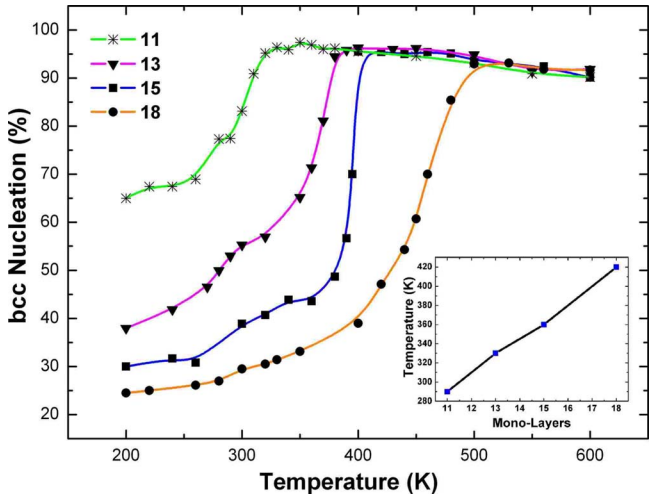

FIG. 7. (Color online) Percentage of bcc-nucleated atoms as function of temperature, after deposition of 11, 13, 15, and 18 ML of Cu on Au. Interface and top-layer atoms were not taken into account since the AJM could not identify them. The inset presents the transition temperature of the bcc to bct as function of the thickness.

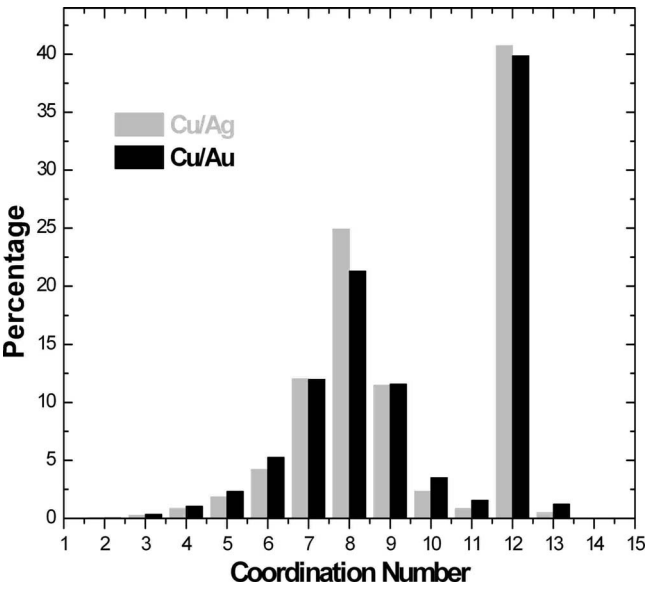

FIG. 8. Distribution displaying coordination numbers of all atoms in the system Cu on Ag (gray) and Cu on Au (black). The histograms show distributions centered at coordination numbers 8 (bct Cu) and 12 (fcc Ag/Au).

Cu/Ag. The Cu/Ag has also presented a more defined pattern (see Figs. 4 and 6). This can be explained in terms of the elastic constants of both substrates. The elastic constants c_{11} and c_{12} used to fit the EAM potential are linearly related to the normal compressive strain in the [001] direction. These constants present significantly larger values for Au than for Ag. In ergs/cm^3 these values are $c_{11}=1.83$ for Au and $c_{11}=1.29$ for Ag, and $c_{12}=1.59$ for Au and $c_{12}=0.91$ for Ag. Therefore, when the stress is relaxed in the Au substrate, less deformations occur compared to the case of Ag since Au has larger elastic constants related to the surface-normal compressive strain. Note that the deformation propagates also into the film. After relaxing the stress there is a spatial dependence of the ratio c/a in the film with a strain variation (see Fig. 3). The smaller variation in the normal compressive strain along [001] occurred for the Cu/Au system, which confirms our understanding that a less deformed system gives a modulation pattern with shorter period and less defined than the Cu/Ag as can be observed by comparing Figs. 4 and 6.

C. Relation of temperature, film thickness, and bcc/bct structures

The bcc nucleation curves as function of temperature were studied similarly to the previous case. For the Cu/Au system results are displayed in Fig. 7, which shows the temperature dependence of films with 11, 13, 15, and 18 deposited monolayers on Au(001). Analogous to the case of Cu on Ag, the lattice parameters a and b of deposited Cu on Au(001) expand following the substrate. But as thickness grows, a and b tend to relax and shorten, while c increases, with the structure searching for its energy minima. This suggests that upon deposition of many layers the Cu film evolves to the fcc phase, the most stable Cu structure found in nature. We have also found that if the thickness is smaller, say 11 or 13 ML, the bcc ratio of nucleated atoms is higher as compared with thicker films. For example, films with 15 or 18 ML at the same temperature show a smaller bcc ratio. bcc nucleation occurs for lower temperatures in accordance with the interpretation that pseudomorphic growth for layers close to the substrate guarantees the tensile stress along a and b and relaxation of c from the substrate. With the deposition of many monolayers the quantity of bcc-nucleated atoms varies significantly depending on the film temperature, in accordance with the lowering of tensile stress with the increment of the number of deposited layers. This can be seen if we compare the line for the case of 11 ML with that of 18 ML. The curve for the film with 11 ML shows the bcc nucleation of 65% at 200 K, quite different from the case of 18 ML, where only 25% of the atoms showed bcc nucleation at this temperature. In the intermediate case of 15 deposited layers at temperature of 400 K, the majority of the Cu atoms (95.5%) have bcc nucleation; but as temperature is lowered below 380 K, a severe drop in bcc nucleation occurs, giving a value for the bcc nucleation of 48.7%. At this same temperature, the bcc nucleation for 13 ML was 94.5%. The behavior of the bcc nucleation can be clearly observed in Fig. 7. The inset shows the transition temperature as function of the number of layers.

D. Coordination number and first-neighbor distance

A procedure to distinguish atoms by their coordination numbers was used to analyze the films studied. The cutoff radius of 2.63 Å was used for both systems. In the case of Cu on Ag, the Cu film with 15 ML at 360 K showed the majority (88.7% of the total deposited Cu atoms) of its atoms with coordination numbers between 7, 8, and 9, a distribution around 8 which can be understood in terms of Bain

distortions of the lattice and temperature effects. The same procedure applied to Cu on Au gave similar results. A histogram with the percentage of atoms (substrate and deposited film) as function of coordination number for both systems is presented in Fig. 8. We can see from the distributions of the number of neighbors a clear distinction of Cu film (bcc) and substrate (fcc) in the histogram. We noted that distortions occurred around coordination numbers 8 and 12, representative of bcc Cu film and fcc Ag and Au substrates. The average first-neighbor distance was calculated as 2.5 Å for Cu on Ag and 2.53 Å for Cu on Au.

V. CONCLUSIONS AND PERSPECTIVES

In this paper we used computer simulations to show that it is possible to model atomic deposition of metal films on metal substrates using classical molecular dynamics with very reliable results. We studied the growth of Cu thin films on Ag(001) and Au(001). On those substrates Cu undergoes a martensitic transformation and forms in bcc and bct structures, in agreement with previous experimental results. We hope that our model contributed to the understanding of the phenomena showing qualitatively as well as quantitatively that the formation of bcc and bct structures is related to temperature and thickness of the thin film, as discussed in Secs. III C and IV C. We also calculated the periods of stripe formation to be 57 Å for Cu/Ag and 61 Å for Cu/Au and also the Cu interlayer distances {001} that changed to 1.41 Å, evidencing the pseudomorphic growth with the substrate lattice. The methodology used here is reliable and can be extended to study deposition of other metallic films on metallic substrates. It could also be used to study film growth and other properties in different types of systems such as semiconductors provided an appropriate interatomic potential is used.

ACKNOWLEDGMENTS

Simulations were performed at the Centro Nacional de Computacao de Alto Desempenho (CENAPAD-SP) and at the Institute of Physics "Gleb Wataghin" (IFGW), both in São Paulo. This work was supported by Fundacao de Amparo a Pesquisa do Estado de São Paulo (FAPESP) and Conselho Nacional de Desenvolvimento Cientifico e Tecnologico (CNPq). Z.S.P. thanks CNPq for a research grant and also thanks Rickson Mesquita for helpful discussions on the paper.

[1] E. C. Bain, Trans. AIME **70**, 25 (1924).
[2] B. M. Ocko, I. K. Robinson, M. Weinert, R. J. Randler, and D. M. Kolb, Phys. Rev. Lett. **83**, 780 (1999).
[3] R. J. Randler, D. M. Kolb, B. M. Ocko, and I. K. Robinson, Surf. Sci. **447**, 187 (2000).
[4] M. Dietterle, T. Will, and D. M. Kolb, Surf. Sci. **396**, 189 (1998).
[5] E. Hahn, E. Kampshoff, N. Wälchli, and K. Kern, Phys. Rev. Lett. **74**, 1803 (1995).
[6] J. R. Chelikowsky and M. Y. Chou, Phys. Rev. B **38**, 7966 (1988).
[7] T. Kraft, P. M. Marcus, M. Methfessel, and M. Scheffler, Phys. Rev. B **48**, 5886 (1993).
[8] A. M. Bittner, J. Wintterlin, and G. Ertl, Surf. Sci. **376**, 267 (1997).
[9] W. Obretenov, U. Schmidt Muller, W. J. Lorenz, G. Staikov, E. Budevski, D. Carnal, U. Müller, H. Siegenthaler, and E. Schmidt, J. Electrochem. Soc. **140**, 692 (1993).
[10] S. J. Plimpton, J. Comput. Phys. **117**, 1 (1995).
[11] M. S. Daw and M. I. Baskes, Phys. Rev. Lett. **50**, 1285 (1983).
[12] M. S. Daw and M. I. Baskes, Phys. Rev. B **29**, 6443 (1984).
[13] S. M. Foiles, M. I. Baskes, and M. S. Daw, Phys. Rev. B **33**, 7983 (1986).
[14] G. J. Ackland and A. P. Jones, Phys. Rev. B **73**, 054104 (2006).
[15] M. I. Haftel, M. Rosen, T. Franklin, and M. Hettermann, Phys. Rev. B **53**, 8007 (1996).
[16] J. A. Sprague, F. Montalenti, B. P. Uberuaga, J. D. Kress, and A. F. Voter, Phys. Rev. B **66**, 205415 (2002).
[17] L. A. Bruce and H. Jaeger, Philos. Mag. **36**, 1331 (1977).
[18] P. Hohenberg and W. Kohn, Phys. Rev. **136**, B864 (1964).
[19] M. J. Stott and E. Zaremba, Phys. Rev. B **22**, 1564 (1980).
[20] J. Cai and Y. Y. Ye, Phys. Rev. B **54**, 8398 (1996).
[21] C. Vailhe and D. Farkas, J. Mater. Res. **12**, 2559 (1997).
[22] W. G. Hoover, Phys. Rev. A **31**, 1695 (1985).
[23] L. D. Landau and E. M. Lifshitz, *Theory of Elasticity* (Pergamon, New York, 1970).